

Scanning Electron Microscopy and Fourier Transformed Infrared Spectroscopy Analysis of Bone Removal Using Er:YAG and CO₂ Lasers

Katia M. Sasaki,* Akira Aoki,* Shizuko Ichinose,† Toshiaki Yoshino,* Sachiko Yamada,‡ and Isao Ishikawa*

Background: A thorough analysis of laser-ablated bone tissue is required before applying the technique to osseous surgery. In this study, we examine the morphological features and chemical composition of the bone surface after Er:YAG and CO₂ lasers ablation.

Methods: Six Wistar rats were used. An Er:YAG laser was used for ablation at an output energy of 100 mJ/pulse and a pulse rate of 10 Hz (1 W). Continuous CO₂ laser irradiation was performed at an output energy of 1 W. Sites drilled using a conventional micromotor were used as controls. Analysis using scanning electron microscopy (SEM) and Fourier transformed infrared (FTIR) spectroscopy was performed.

Results: Er:YAG laser ablation produced a groove with similar dimensions to that produced by bur drilling, whereas the CO₂ laser produced only a charred line with minimal tissue removal. SEM observations revealed that the groove produced by the Er:YAG laser had well-defined edges and a smear layer-free surface with a characteristically rough appearance and with entrapped fibrin-like tissue. The melting and carbonization produced by the CO₂ laser were not observed on sites irradiated by the Er:YAG laser. FTIR spectroscopy revealed that the chemical composition of the bone surface after Er:YAG laser ablation was much the same as that following bur drilling. The production of toxic substances that occurred after CO₂ laser irradiation was not observed following Er:YAG laser irradiation or bur drilling.

Conclusion: These results suggest that the use of Er:YAG laser ablation may become an alternative method for oral and periodontal osseous surgery. *J Periodontol* 2002;73:643-652.

KEY WORDS

Bone and bones/anatomy and histology; laser surgery; comparison studies.

Ever since Mainman developed the ruby laser in 1960,¹ there has been a continuous development of laser applications in medical fields. Studies on bone cutting using lasers have typically focused on the use of CO₂ lasers in both continuous-wave and rapid superpulsed modes.²⁻⁵ Recently, however, the Er:YAG laser has been recognized as a promising tool for bone ablation in orthopedic and otolaryngology surgery.⁶⁻¹⁰ Similarly, recent research in dentistry has revealed the potential applicability of the Er:YAG laser to dental hard-tissue ablation, such as enamel and dentin removal,¹¹⁻¹⁴ and the suitability of the Er:YAG laser as an alternative for non-surgical periodontal treatment was recently reported by Schwarz et al.¹⁵ The application of this laser for bone ablation in oral and periodontal surgery is an expected step; however, there are only few reports regarding the use of Er:YAG lasers in bone surgery and little is known about the effectiveness of the Er:YAG laser for bone ablation or the characteristics of the irradiated bone tissue compared to conventional dental rotary instruments. The present study was conducted in order to clarify this issue, by comparing the effectiveness of bone tissue removal and the morphological and chemical features of the bone surface treated by Er:YAG and CO₂ lasers with those drilled using a low-speed rotary bur. Treated samples were examined by scanning electron microscopy (SEM) and Fourier transformed infrared (FTIR) spectroscopy.

* Division of Periodontology, Department of Hard Tissue Engineering, Graduate School, Tokyo Medical and Dental University, Tokyo, Japan.

† Instrumental Analysis Research Center.

‡ Institute of Biomaterials & Bioengineering.

MATERIALS AND METHODS

Experimental Animals and Surgical Access Design

Six 10-week-old male Wistar rats were used in this experiment. The rats were first sedated using diethyl ether and then anesthetized with an intraperitoneal injection of ketamine hydrochloride (100 mg/kg). The backs of the animals were then shaved using electric clippers and disinfected with 70% ethanol solution. The dorsal skin at the neck was incised, elevated, and dissected to expose the underlying calvaria region. Then, 3 distinct incisions were made with a scalpel blade in the periosteum of the calvaria. The first incision (1.5 cm long) was made at the neck transversally to the body axis. Two other parallel incisions (2 cm length each) were made from the end of each side of the first incision towards the eyes. The periosteum was then gently elevated to expose the parietal bone surfaces.

This animal experiment was performed in accordance with a protocol that satisfies the ethical standards of the Animal Research Center of the Tokyo Medical and Dental University.

Study Design

SEM observation. Four rats were used for SEM analysis. After bone exposure, the parietal bones were treated as shown in Figure 1A. The lower sites (nearer the neck) of both the right and left parietal bones were irradiated by the Er:YAG laser. The upper sites (nearer the eyes) of the right parietal bone and the left parietal bone were treated with a bur drill and CO₂ laser, respectively. Each instance of laser irradiation and bur drilling was performed in a single pass creating a 5 mm long line at each site. The time required for bur drilling and Er:YAG laser ablation was approximately 3 seconds, while CO₂ laser irradiation took approximately 2 seconds.

FTIR analysis. The other 2 rats were used for FTIR spectroscopy. The frontal and parietal bones were exposed and the skin around the treated area was removed. The entire exposed area was divided into 6 parts as shown in Figure 1B. Each part was treated by either Er:YAG laser, CO₂ laser, or bur drilling with sweeping movements for approximately 20, 15, and 20 seconds, respectively, in order to obtain approximately 3 × 4 mm of each treated area. The 2 remaining parts of the frontal bone were used as control material.

Laser Characteristics

The Er:YAG laser used in this experiment was a pulsed Er:YAG laser,[§] with a wavelength of 2.94 μm, an output range of 30 to 350 mJ/pulse, a maximum pulse repetition rate of 10 Hz, and a pulse duration of 200 μs. The CO₂ laser^{||} was a continuous-wave CO₂ gas laser with a wavelength of 10.6 μm and an output range of 0.5 to 5 W. The micromotor[¶] used for bur drilling was a standard low-speed dental micromotor with a straight handpiece.

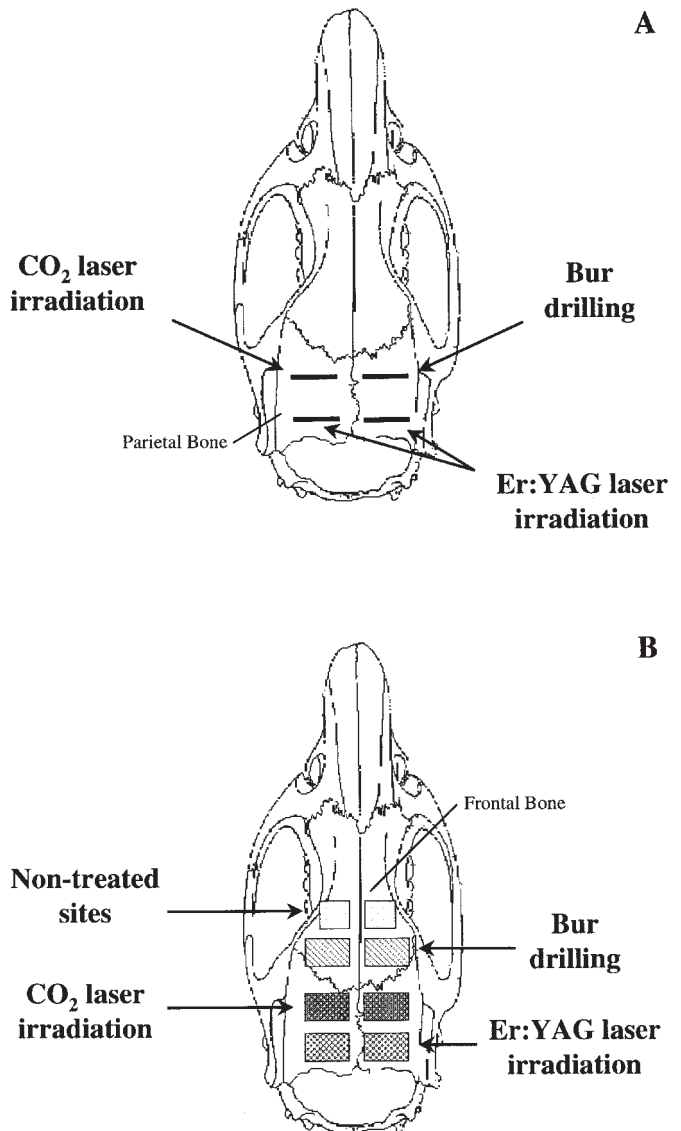


Figure 1.

Schematic location of treated sites on rat calvaria. **A.** SEM observation, single pass of laser beam and steel bur creating a 5 mm long line at each site. **B.** FTIR analysis, 2 treated sites of approximately 3 × 4 mm were created for each treatment mode. Irradiation was performed with sweeping movements for approximately 5 seconds for CO₂ laser irradiation and approximately 10 seconds for both bur drilling and Er:YAG laser irradiation. The remaining portion of the frontal bone was used as control material.

Laser Irradiation and Bur Drilling Conditions

The energy output of the Er:YAG laser was 100 mJ/pulse, used at a pulse repetition rate of 10 Hz (1 W). The energy setting on the control panel was adjusted by measuring the output power at the tip of the con-

§ ML22, Erwin, HOYA Continuum Corp., Tokyo, Japan and J. Morita Mfg. Corp., Kyoto, Japan.

|| Opelaser-03S, Yoshida Co. Ltd., Tokyo, Japan.

¶ Beaver II, Osada Electric Co. Ltd., Tokyo, Japan.

tact probe using a power meter.[#] This energy setting was selected considering the results of our pilot experiment, where an energy output of 100 mJ/pulse was considered to be clinically appropriate for effective bone ablation (unpublished data). Lower energies could not efficiently remove bone tissue. Higher energies presented minimally higher efficiency in contrast to other clinical parameters, such as preciseness, patient comfort, and machine wear and tear. Also, we considered the suitable range of energy setting for dentin ablation reported in our previous work.¹⁶ For the CO₂ laser, we opted to use similar output settings in the present study, since carbonization would occur even using the lowest settings and higher outputs would cause even worse effects. Er:YAG laser irradiation was performed at an incident angle of approximately 30° to the moistened surface in contact mode under saline solution irrigation. CO₂ laser irradiation was performed with the same energy output (1 W), in focused non-contact mode, 2 to 5 mm from the target surface, using an aimed laser beam. Bur drilling was performed using a round steel bur^{**} operated at 10,000 rpm. The bur was held at an angle of approximately 30° to the bone surface. Saline solution irrigation was performed using a disposable syringe for both Er:YAG laser irradiation and bur drilling. No water coolant was used during CO₂ laser ablation because, as we observed in our pilot study, the CO₂ laser performance is impaired when water is applied (unpublished data).

Specimen Preparation

After the surgical procedures, the animals were sacrificed by decapitation. The calvaria were dissected and trimmed using a bandsaw^{††} under saline solution irrigation. The calvaria specimens were thoroughly washed with saline solution using a disposable syringe in order to remove blood clots from the treated sites.

SEM observation. Four specimens were pre-fixed for 2 hours in 2.5% glutaraldehyde fixative solution and then rinsed overnight with 0.1 M phosphate buffer solution. The specimens were post-fixed with 1% osmium tetroxide for 2 hours, and dehydrated in a series of graded ethanol solutions. After being washed with 3-methylbutylacetate and then dried to the critical point,^{‡‡} the specimens were attached to an aluminum mount and coated with 4 nm of osmium plasma coater.^{§§} The specimens were then observed in a scanning electron microscope^{|||} at 15 kV, from 50 to 100,000× magnification.

FTIR analysis. The potassium-bromide (KBr) method was employed, as described previously.¹⁷ The surface of each treated site was scraped gently using the tip of a scalpel blade. The scraped powder was placed on a solid KBr plate (7 × 7 × 1 mm) cut from a KBr block,^{¶¶} and then covered with another KBr plate. The sandwiched sample was then pressed at

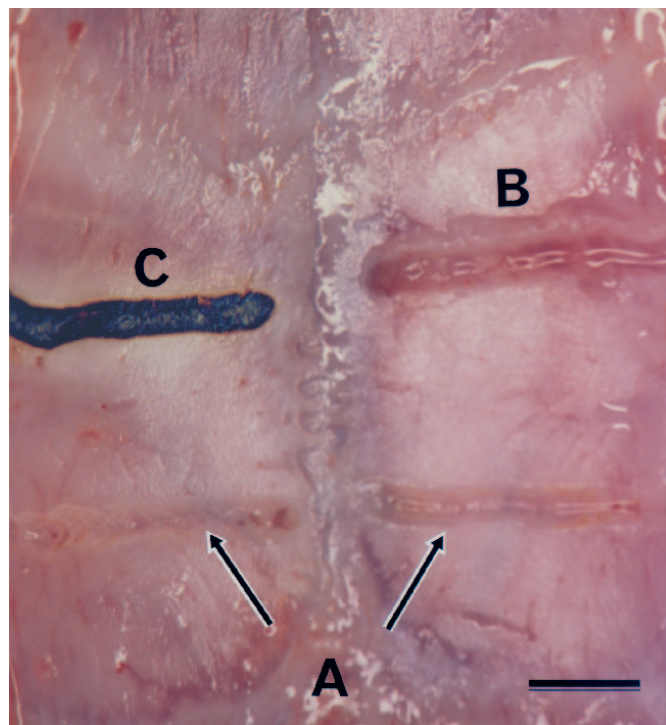


Figure 2.

Clinical view of treated bone surface after Er:YAG laser irradiation (A), bur drilling (B), and CO₂ laser irradiation (C). Er:YAG laser irradiation was performed at 100 mJ/pulse and 10 Hz (1 W) under saline solution irrigation in contact mode at an incident angle of 30° to the surface. Bur drilling was performed at an angle of 30° to the surface under saline solution irrigation. CO₂ laser irradiation was performed at 1 W continuous wave without irrigation, in focused non-contact mode. Note that the carbonization observed due to CO₂ laser irradiation did not occur due to Er:YAG laser irradiation (bar = 2 mm; original magnification ×2).

180 Kg/cm² at room temperature using a gas compressor,^{##} producing a round compressed pellet with a diameter of 10 mm for each treatment site. The pellet was then analyzed in the FTIR spectrometer.^{***} The spectra were recorded at standard 8 cm⁻¹ resolution with a spectral range of 650 to 4000 cm⁻¹.

RESULTS

Figure 2 shows the clinical appearance of the treated bone surface. Er:YAG laser irradiation produced a groove with precise edges. Irradiation by the CO₂ laser resulted in a black carbonized line with a whitish part in the center and only minor tissue removal, and bur

Field master, Coherent, Santa Clara, CA.

** ISO 006, Meisinger, Dusseldorf, Germany.

†† K-100, Hozan Tool Industrial Co., Ltd., Osaka, Japan.

‡‡ HCP-2 Critical point drier, Hitachi Ltd., Hitachinaka, Japan.

§§ Osmium plasma coater OPC 80, Nippon Laser and Electronics, Nagoya, Japan.

||| S-4500, Hitachi Ltd., Japan.

¶¶ Wako Pure Chemical Industries, Ltd., Osaka, Japan.

Riken Power, Riken Seiki Co. Ltd., Niigata, Japan.

*** Janssen Micro FTIR spectrometer, Japan Spectroscopic Company, Tokyo, Japan.

drilling produced a pinkish groove. During CO₂ laser irradiation, a strong smell of charring was noticed despite the use of dental suction.

SEM Observations

Er:YAG laser. Er:YAG laser irradiation produced a groove with well-defined edges similar to that produced by bur drilling. The groove itself was made up of a series of craters (Fig. 3A). At higher magnifications, the numerous multilayered projections could be seen, resulting in a rough scaly appearance (Fig. 4A). Fibrin-like tissue was frequently entrapped in these projections (Figs. 5A and 6) after Er:YAG laser treatment. This phenomenon was not observed in either bur-drilled or CO₂ laser-irradiated surfaces (Fig. 5B and 5C). At ultra-high magnifications, each projection was seen to be composed of fibrous structures surrounded by round microparticles. Numerous small spaces existed among the microparticles and the fibers, comprising a porous surface (Fig. 7A). Another feature of Er:YAG laser

ablation was seen at high magnification, as shown in Figure 7B, where enlarged round fusions of particles can be seen among the many isolated microparticles. The parched fibers and larger spaces between microparticles give the surface a brittle aspect.

Bur drilling. Figure 3B shows the groove created by bur drilling. The groove is essentially smooth with periodic bur round marks. A remnant of soft tissue could be seen on one margin of this groove; this was not seen in any of the other treatments. At higher magnification, numerous linear tracks obliquely displayed and covered by smear layer can also be seen (Fig. 4B). At ultra-high magnification, the smear layer appears homogeneous, composed of densely packed microparticles (Fig. 8A). Where less smearing was present, small particles surrounded by abundant collagen fibers and tissue matrix were observed (Fig. 8B).

CO₂ laser ablation. CO₂ laser irradiation resulted in minimal tissue removal and no distinct groove was created. The irradiated site showed merely a cracked

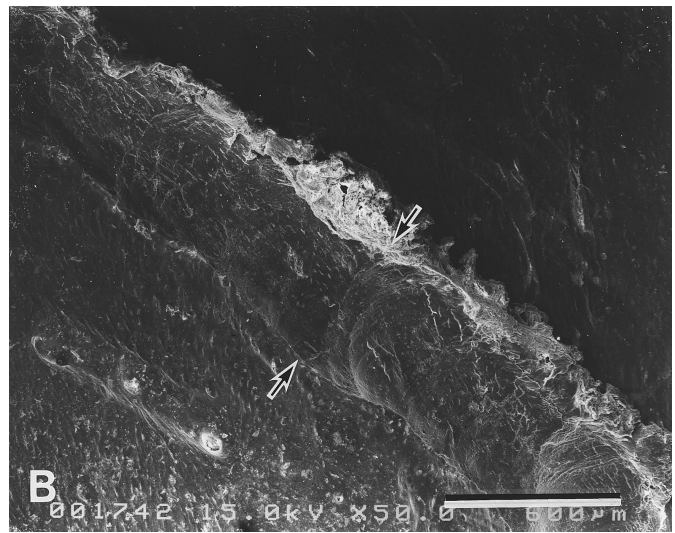
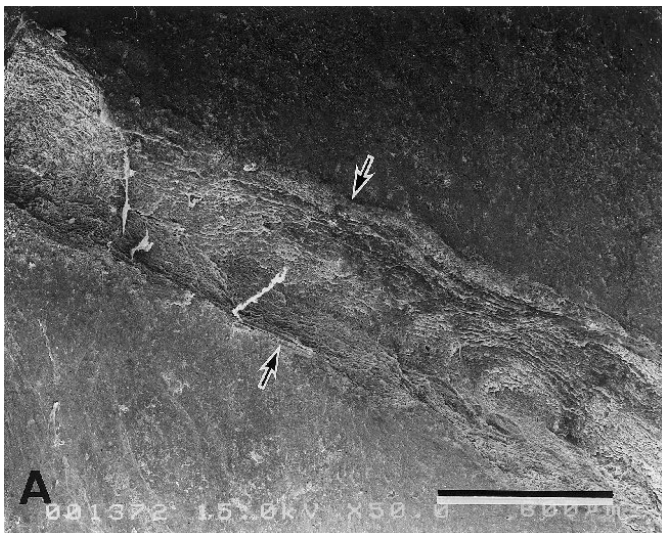


Figure 3.

Low-magnification SEM photomicrographs. **A.** Er:YAG laser ablation; **B.** bur drilling; and **C.** CO₂ laser ablation. Note the groove-like appearance of the bone surface after Er:YAG laser irradiation and bur drilling; and the cracked appearance of the bone surface after CO₂ laser irradiation. The arrows identify the treated surface (bar = 600 μm; original magnification ×50).

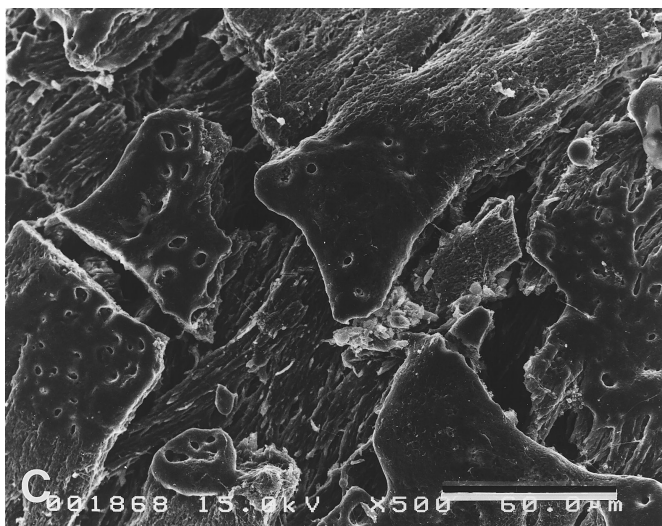
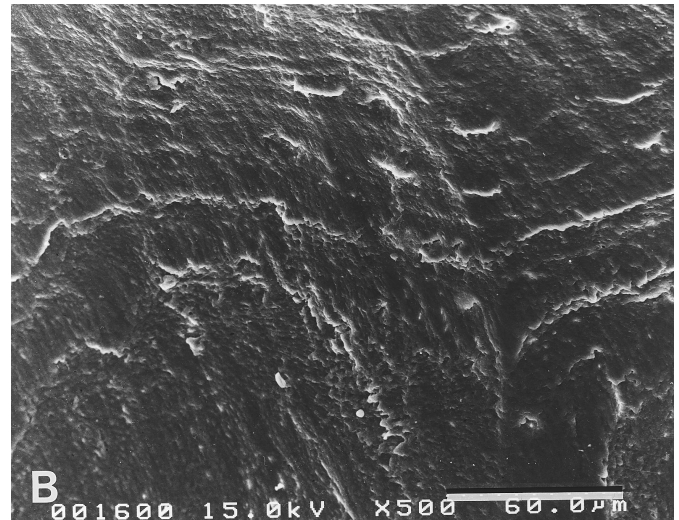
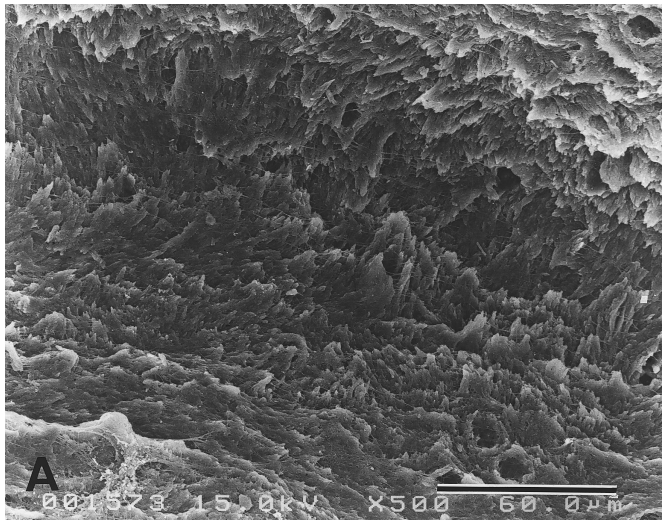


Figure 4.

Low-magnification SEM photomicrographs of bone surface after Er:YAG laser ablation (A), bur drilling (B), and CO₂ laser ablation (C). Note the numerous projections produced by Er:YAG laser ablation, the smear layer-covered appearance of the bone surface after bur drilling, and the melted and cracked appearance of the bone surface after CO₂ laser irradiation (bar = 60 µm; original magnification x500).

surface, with a broad thermally damaged zone observed as a darker area surrounding the irradiated line (Fig. 3C). At higher magnification, the surfaces appeared melted and resolidified, with no smear layer (Fig. 4C). The resolidified sites presented completely fused structures (Fig. 5C). At ultra-high magnification, 2 typical features of CO₂ laser irradiation could be seen: the surface is formed of groups of large round particles (Fig. 9A), and the fusion of particles in a dense mass of tissue with numerous lacunas on the surface (Fig. 9B). No collagen fibers were observed at these sites.

FTIR Spectra

The spectra for untreated bone showed orthophosphate, carbonate, amides, and hydroxyl group bands. Small peaks were observed in the 2340 cm⁻¹ region, corresponding to molecular CO₂. The orthophosphate and carbonate bands represent mainly the inorganic content of the specimen. The amide bands indicate the presence of proteins. The hydroxyl band is related

to water and also to the organic content. The orthophosphate groups were recorded in the absorption band between 1030 and 1150 cm⁻¹, the carbonate bands were present at around 875 cm⁻¹ and between 1560 and 1410 cm⁻¹, the amide bands were observed between 1680 and 1200 cm⁻¹, and the OH group absorption band was observed between 3600 and 2400 cm⁻¹. The amide bands were divided in the amide I band between 1680 and 1600 cm⁻¹, the amide II band between 1580 and 1480 cm⁻¹, and the amide III band between 1300 and 1200 cm⁻¹ (Fig. 10A).

The bands in the spectra for the Er:YAG laser-ablated specimens with water irrigation were similar to those for the untreated specimens except for the decrease of amide I and OH bands compared to orthophosphate bands. The profile was otherwise basically identical, and no additional bands were observed (Fig. 10B).

The spectra for the bur-drilled specimens also exhibited the same bands as the untreated specimen (Fig. 10C).

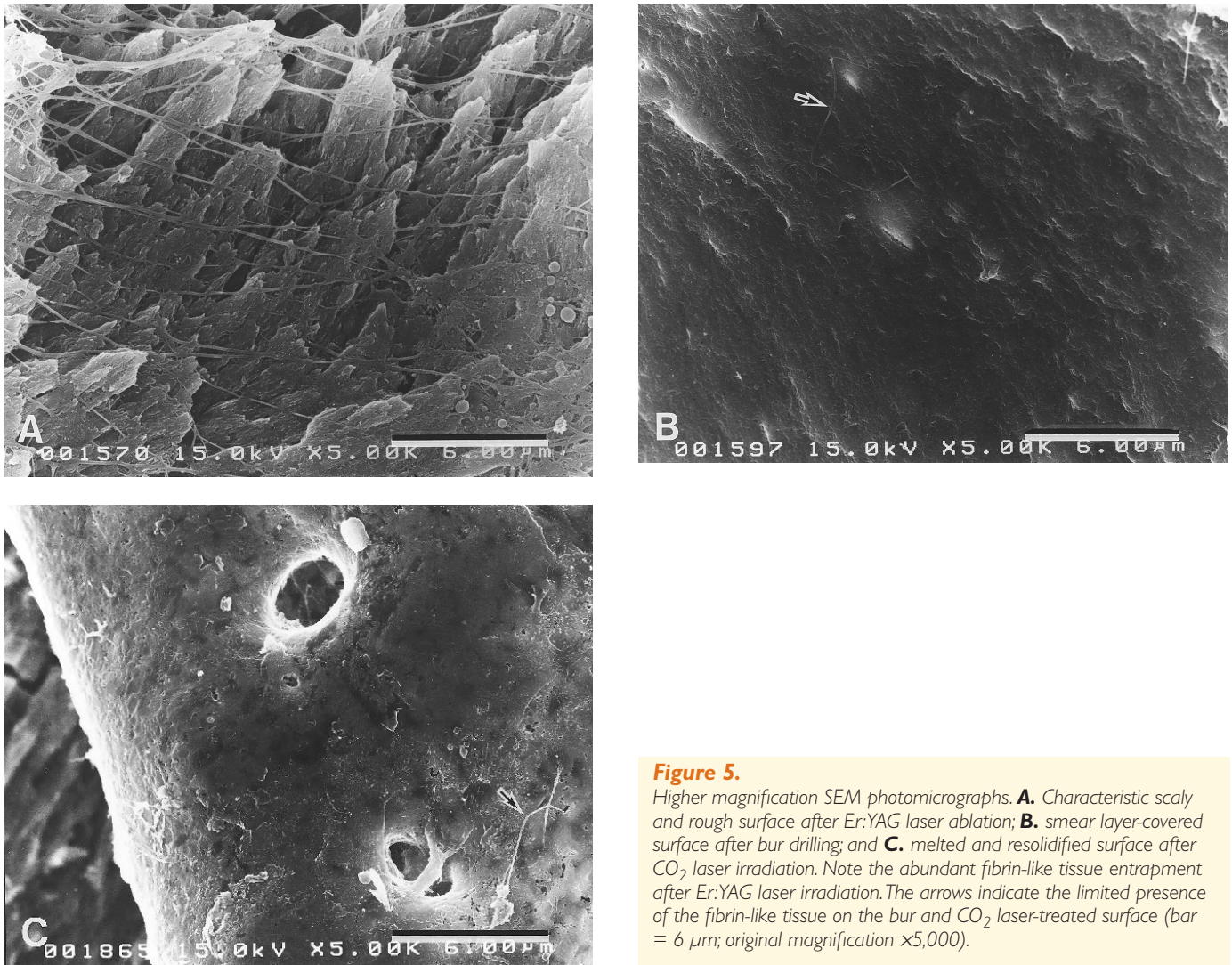


Figure 5.

Higher magnification SEM photomicrographs. **A.** Characteristic scaly and rough surface after Er:YAG laser ablation; **B.** smear layer-covered surface after bur drilling; and **C.** melted and resolidified surface after CO₂ laser irradiation. Note the abundant fibrin-like tissue entrapment after Er:YAG laser irradiation. The arrows indicate the limited presence of the fibrin-like tissue on the bur and CO₂ laser-treated surface (bar = 6 µm; original magnification x5,000).

The spectra for the CO₂ laser-irradiated specimens were clearly different from all the other groups; the amide peaks had almost entirely disappeared leaving only a very small amide I band, and while the carbonate band between 1560 and 1410 cm⁻¹ remained, the OH band was also significantly weakened. Two additional absorption bands were present at 2200 and 2010 cm⁻¹ related to cyanate (NCO⁻) and cyanamide (NCN²⁻) ions, respectively.¹⁸ The carbonate peak at 875 cm⁻¹ was also noticeable (Fig. 10D).

DISCUSSION

The principles of osseous surgery in periodontal disease therapy were first outlined by Schluger.¹⁹ Subsequently, Friedman²⁰ and Ochsenbein²¹ reported that, wherever possible, the bony architecture should be restored when such architecture was destroyed by periodontal disease. Since then, alveolar bone recontouring and reshaping have been used in periodontal therapy to establish the physiologic anatomy of the alveolar bone that allows an optimal gingival contour after

surgery. Currently, alveolar bone is recontoured when neither the supporting bone nor any further regenerative therapy is compromised.²² For these procedures, rotary instruments such as carbide and diamond burs and hand instruments such as chisels and bone files have been used. Sharp bone chisels reportedly cause the least tissue damage and should be employed whenever access allows.²³ Where access is limited, the use of surgical burs or files is suggested.²² However, mechanical instrumentation is not always feasible in the molar area. Furthermore, use of rotary instruments may occasionally involve the surrounding soft tissue such as reflected flaps and may damage the tooth when supporting bone is to be removed or beveled near the root surface.²¹ The healing rate following drilling has also been reported to be lower than for chisels.²³ Considering the weaknesses of the instruments for bone cutting widely used at present, laser devices are expected to become adjunctive or alternative tools for easier and more precise bone surgery procedures.²⁴

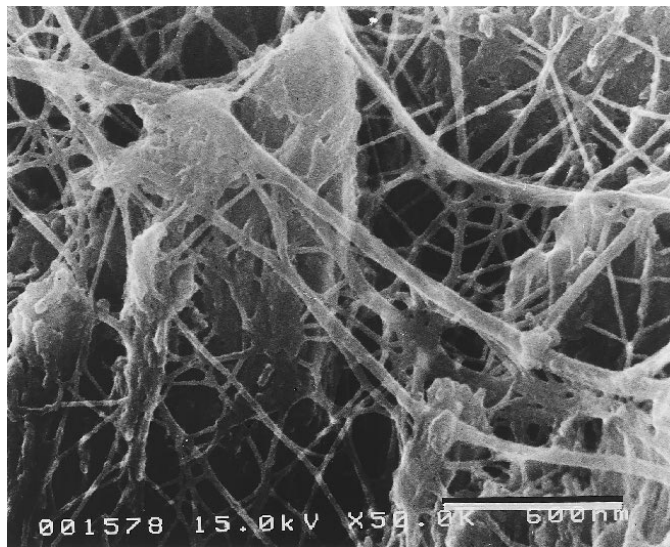


Figure 6.

Higher magnification SEM photomicrograph. Detail of the fibrin-like tissue entrapment observed after Er:YAG laser irradiation (bar = 600 nm; original magnification $\times 50,000$).

In this study, we demonstrated the bone cutting ability of the Er:YAG laser, with results comparable to that of conventional steel burs. The groove-like appearance of both Er:YAG laser-ablated and bur-drilled surfaces clearly illustrates the high suitability of Er:YAG laser ablation for the removal of hard tissue. Moreover, the well-defined edges of the groove obtained by Er:YAG laser ablation are indicative of the accuracy of this tool for such procedures. In contrast, the use of a CO₂ laser at an output energy of 1 W only resulted in melting and carbonization, without acceptable tissue removal. It is understood that use of a CO₂ laser at higher energy levels would be capable of ablating bone tissue; however, carbonization will still be inevitable. Thus, the use of CO₂ laser for bone ablation procedures is considered to be far less promising than the use of Er:YAG lasers. The time required to achieve a given level of tissue removal by Er:YAG laser ablation is comparable to that of bur drilling. Although the device tested in the present study exhibited acceptable performance, the use of higher repetition rates of the laser pulses may be advantageous in terms of increased efficiency and decreased energy output, with theoretically fewer changes in tissue structure.

In the bur-drilled specimens, some soft tissue remained at one edge of the groove due to the rotational movement of the round bur, a feature not observed on the Er:YAG laser-ablated surfaces. These findings suggest the possibility of Er:YAG laser removal of granulation tissue during periodontal flap surgery.

Lewandrowski et al. reported that the healing rate following Er:YAG laser irradiation may be equivalent

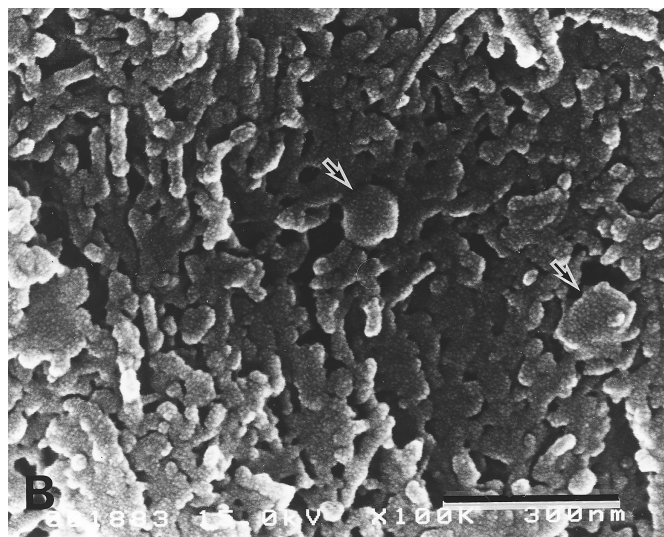
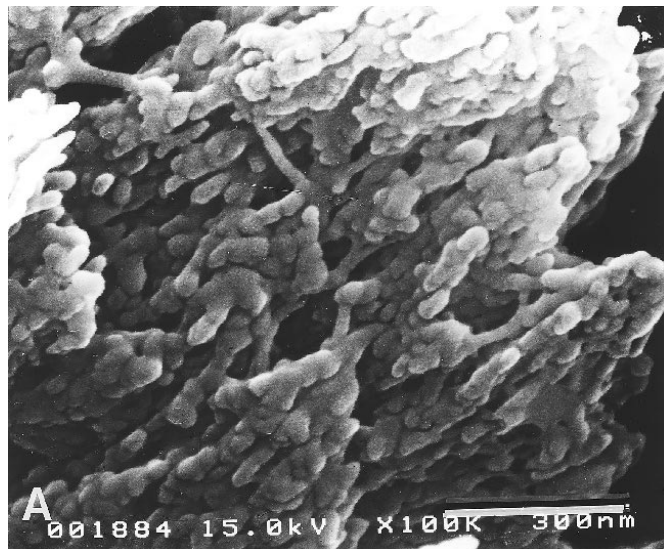


Figure 7.

Ultra-high magnification SEM photomicrographs. **A.** Er:YAG laser-irradiated bone surface composed of a net of fibers surrounded by small round particles. Note the similarity of these structures to those present on the surface after bur drilling in areas where the smear layer is sparse. **B.** Er:YAG laser-irradiated bone surface with enlarged particles (arrows) (bar = 300 nm; original magnification $\times 100,000$).

or even faster than that following bur drilling.²⁵ Although there have been reports of delayed healing following Er:YAG laser ablation,^{26,27} the differences in the results are probably partly due to the use or non-use of water irrigation during ablation, as well as differences in output energy and the surgery design. As we have shown in a previous report on Er:YAG laser ablation of root surfaces without water cooling,¹⁷ not using an air/water coolant during Er:YAG laser irradiation may cause slight charring of the irradiated surface and result in the formation of toxic products. Carbonization and melting of the surface cause the

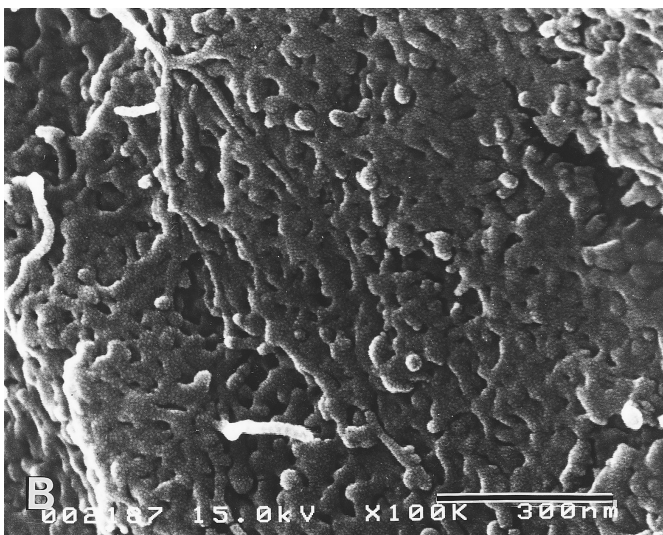
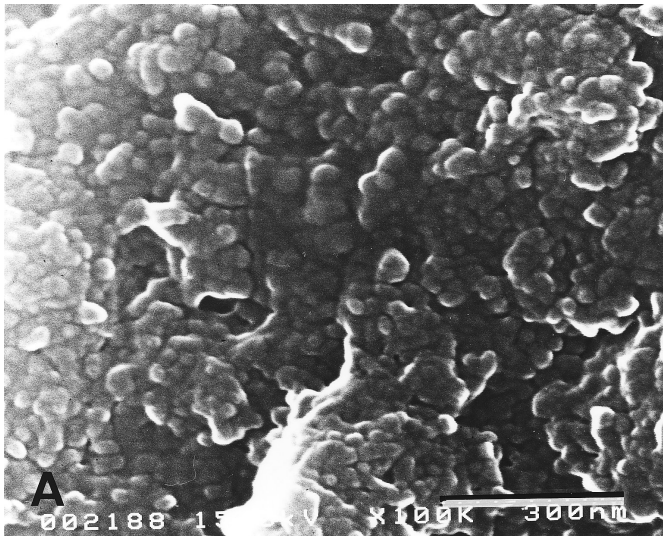


Figure 8.

Ultra-high magnification SEM photomicrographs. **A.** Bur-drilled bone surface covered by a smear layer; **B.** bur-drilled bone surface with sparse smear layer (bar = 300 nm; original magnification $\times 100,000$).

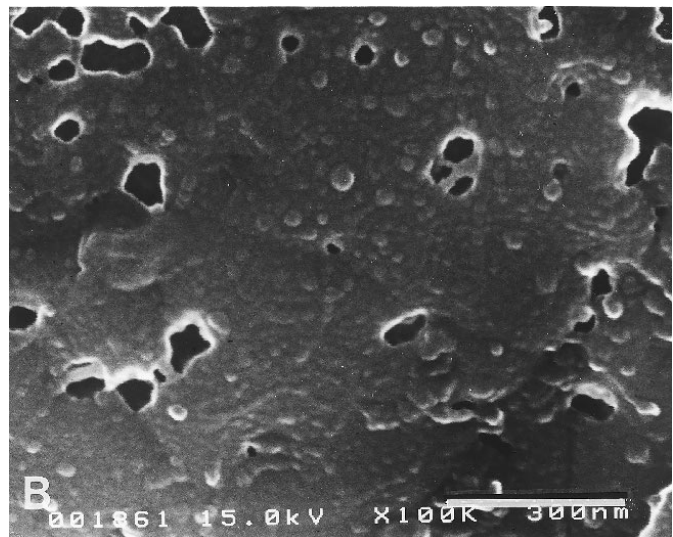
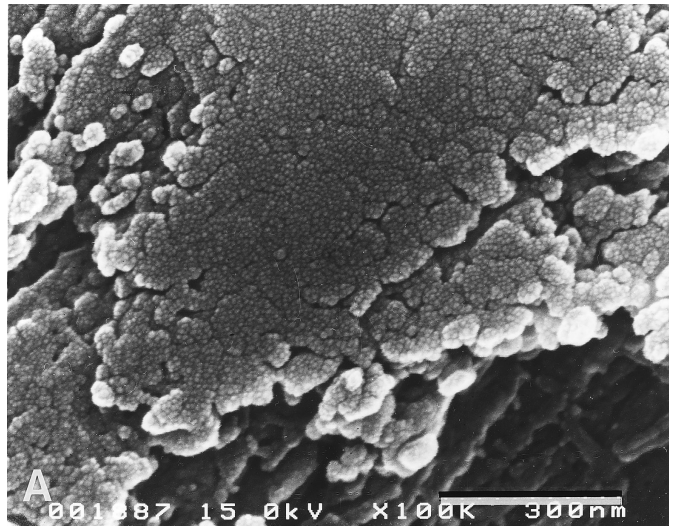


Figure 9.

Ultra-high magnification SEM photomicrographs. **A.** CO₂ laser-irradiated bone surface with groups of enlarged particles; **B.** CO₂ laser-irradiated bone surface with completely melted and refused structures (bar = 300 nm; original magnification $\times 100,000$).

denaturation of proteins by heat, resulting in the formation of toxic byproducts. The formation of these toxic substances was clearly observed in the FTIR spectra obtained for CO₂ laser-irradiated surfaces, and this has been reported as a possible contributor to the delay in the healing process.^{5,28,29} In the case of Er:YAG laser irradiation with coolant, the healing process is expected to be better than that reported after CO₂ laser irradiation because of the lower thermal damage and the absence of toxic by-products.

In this study, the treated bone surfaces presented differences in morphology according to the treatment method which may also influence the healing rate. The surface after bur drilling presented a homogeneous texture covered by a smear layer. The smear layer

may act as a barrier preventing blood element interaction with the underlying tissue, resulting in a delay in the healing process.²³ The Er:YAG laser-treated surface was peculiarly irregular, with entrapment of fibrin-like tissue in the microirregularities. We performed the same experiment *in vitro* using bloodless rat calvaria that had been dissected and stored in formaldehyde solution in order to examine whether the phenomenon was related to the presence of blood immediately after ablation. In this additional experiment, no fibrin-like tissue was observed on the Er:YAG laser-ablated surfaces, or on any of the surfaces treated by the other methods (data not shown). This suggests that the fibrin-like tissue is derived from blood that

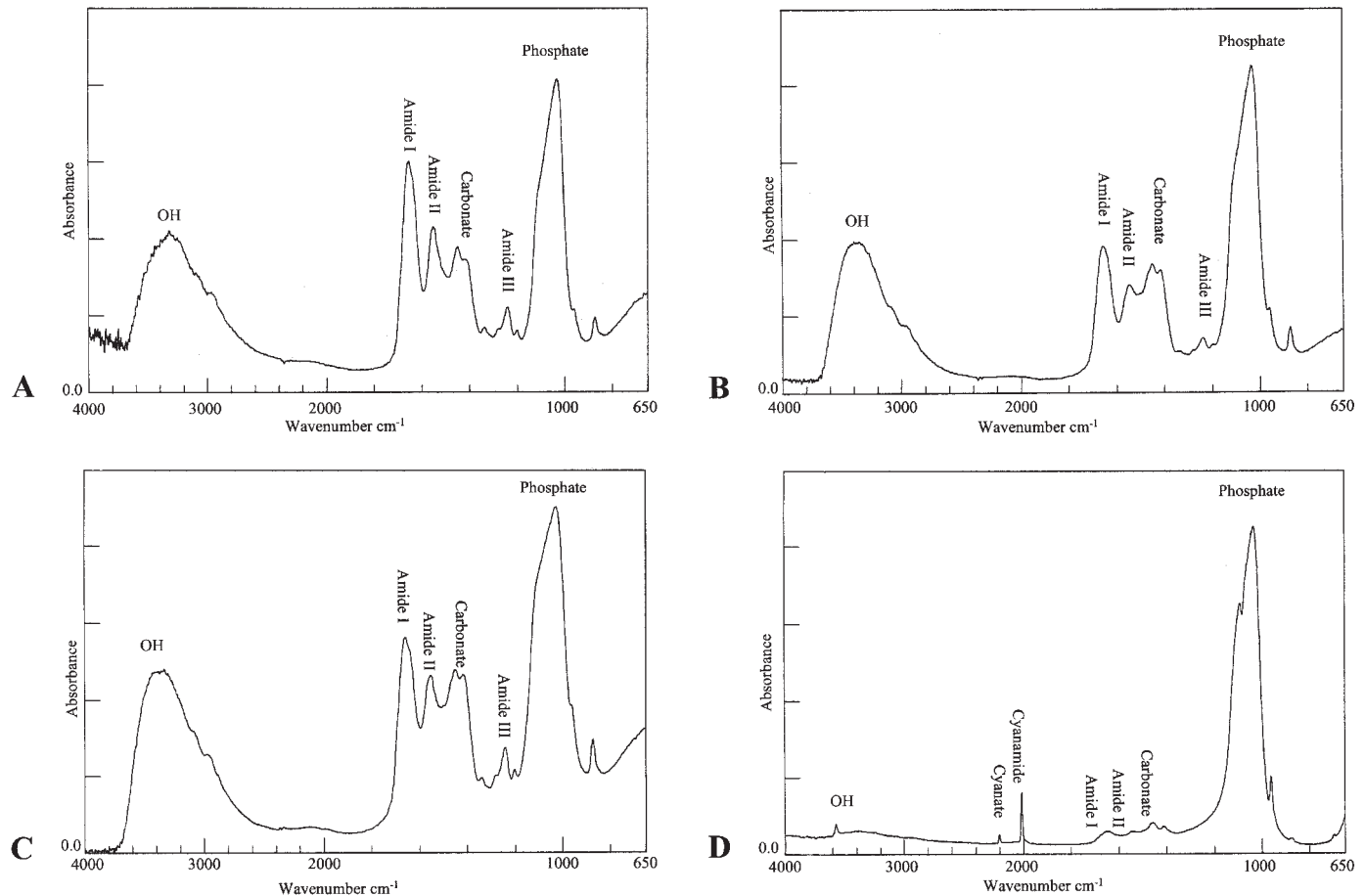


Figure 10.

FTIR spectra of bone surface. **A.** Untreated control specimen; **B.** Er:YAG laser irradiation (100 mJ/pulse, 10 Hz [1 W] under saline solution irrigation); **C.** bur drilling; and **D.** CO₂ laser irradiation (1 W, without coolant). Note the presence of additional new bands in the spectrum for CO₂ laser irradiation (cyanate and cyanamide). Note also the similarity of the spectra for untreated, Er:YAG laser-irradiated, and bur-drilled bone surfaces (A, B, and C).

covers the surfaces after treatment. This tissue could not be removed by saline solution washing when the microprojections were present. The projections might act as a mechanical trap for the plasma proteins and provide the initial basis for fibrin clot adherence. This entrapment may also be caused by contact activation of the intrinsic clotting system by the microprojections.³⁰ However, because the projections revealed some microstructural changes in the SEM observations, the actual effects of Er:YAG laser-ablated structures on the healing process of bone and surrounding tissue will be thoroughly investigated in future studies.

The reduction of the prevalence of collagen fibers among the mineral particles, as observed by SEM at high magnification, is consistent with the present results of FTIR observation and with our previous study where we demonstrated that Er:YAG laser-irradiated surfaces are composed of more inorganic than organic structures, in contrast to untreated surfaces.¹⁷ The enlarged particles and parched fibers may be related

to the large increase in temperature due to Er:YAG laser irradiation, even when water coolant is used, leading to the recrystallization of the bone components, although to a much lesser extent than that due to CO₂ laser irradiation. Although there were virtually no thermally affected areas in the Er:YAG specimens and spectroscopic analysis did not reveal any trace of toxic substances, their effects, if any, during the repair of the bone tissue should also be examined. The actual depth of the layer affected by the Er:YAG laser should also be clarified.

At low SEM magnification, the bone morphology of the specimens was seen to differ quite noticeably according to the treatment methods. At ultra-high magnification, however, the structure of the ablated area in Er:YAG laser-treated specimens appeared to be very similar to that of bur drilling-treated specimens except for the absence of the smear layer. The unique surface produced by Er:YAG laser irradiation may potentially enhance the adhesion of blood elements at the start

of the healing process. The Er:YAG laser exhibited cutting characteristics comparable to bur drills with minimal compositional changes, and is worth considering as an alternative tool for removing and recontouring bone with high precision in osseous surgery.

ACKNOWLEDGMENTS

The authors are indebted to Miss Ojima, of the Instrumental Analysis Research Center of the Tokyo Medical and Dental University and to Ms. Kanauchi, of the JASCO–Japan Spectroscopic Company, Tokyo, for their expert technical assistance.

REFERENCES

- Maiman TH. Stimulated optical radiation in ruby. *Nature* 1960;187:493-494.
- Clauser C. Comparison of depth and profile of osteotomies performed by rapid superpulsed and continuous-wave CO₂ laser beams at high power output. *J Oral Maxillofac Surg* 1986;44:425-430.
- Clayman L, Fuller T, Beckman H. Healing of continuous-wave and rapid superpulsed, carbon dioxide, laser-induced bone defects. *J Oral Surg* 1978;36:932-937.
- Small IA, Osborn TP, Fuller T, Hussain M, Kobernick S. Observations of carbon dioxide laser and bone bur in the osteotomy of the rabbit tibia. *J Oral Surg* 1979;37:159-166.
- Krause LS, Cobb CM, Rapley JW, Killoy WJ, Spencer P. Laser irradiation of bone. I. An in vitro study concerning the effects of the CO₂ laser on oral mucosa and subjacent bone. *J Periodontol* 1997;68:872-880.
- Nuss RC, Fabian RL, Sarkar R, Puliafito CA. Infrared laser bone ablation. *Lasers Surg Med* 1988;8:381-391.
- Nelson JS, Yow L, Liaw LH, et al. Ablation of bone and methacrylate by a prototype mid-infrared erbium:YAG laser. *Lasers Surg Med* 1988;8:494-500.
- Gonzalez C, Van de Merwe WP, Smith M, Reinisch L. Comparison of the erbium-yttrium aluminum garnet and carbon dioxide lasers for in vitro bone and cartilage ablation. *Laryngoscope* 1990;100:14-17.
- Buchelt M, Kutschera HP, Katterschafka T, et al. Erb:YAG and Hol:YAG laser osteotomy: The effect of laser ablation on bone healing. *Lasers Surg Med* 1994;15:373-381.
- Li ZZ, Reinisch L, Van de Merwe WP. Bone ablation with Er:YAG and CO₂ laser: Study of thermal and acoustic effects. *Lasers Surg Med* 1992;12:79-85.
- Hibst R, Keller U. Experimental studies of the application of the Er:YAG laser on dental hard substances: I. Measurement of the ablation rate. *Lasers Surg Med* 1989;9:338-344.
- Hibst R. Mechanical effects of erbium:YAG laser bone ablation. *Lasers Surg Med* 1992;12:125-130.
- Keller U, Hibst R. Experimental studies of the application of the Er:YAG laser on dental hard substances: II. Light microscopic and SEM investigations. *Lasers Surg Med* 1989;9:345-351.
- Kayano T, Ochiai S, Kiyono K, Yamamoto H, Nakajima S, Mochizuki T. Effect of Er:YAG laser irradiation on human extracted teeth. *J Clin Laser Med Surg* 1991;9:147-150.
- Schwarz F, Sculean A, Georg T, Reich E. Periodontal treatment with an Er:YAG laser compared to scaling and root planing. A controlled clinical study. *J Periodontol* 2001;72:361-367.
- Aoki A, Ishikawa I, Yamada T, et al. Comparison between Er:YAG laser and conventional technique for root caries treatment in vitro. *J Den Res* 1998;77:1404-1414.
- Sasaki KM, Aoki A, Masuno H, et al. Compositional analysis of root cementum and dentin after Er:YAG laser irradiation compared with CO₂ lased and intact roots using Fourier transformed infrared spectroscopy. *J Periodont Res* 2002;37:50-59.
- Dowker SEP, Elliot JC. Infrared absorption bands from NCO⁻ and NCN²⁻ in heated carbonate-containing apatites prepared in the presence of NH₄⁺ ions. *Calcif Tissue Int* 1979;29:177-178.
- Schluger S. Osseous resection, a basic principle in periodontal surgery. *Oral Surg Oral Med Oral Pathol* 1949;2:316-325.
- Friedman N. Periodontal osseous surgery: Osteoplasty and ostectomy. *J Periodontol* 1955;26:257-269.
- Ochsenbein C. Osseous resection in periodontal surgery. *J Periodontol* 1958;29:15-26.
- Wennström J, Heijl L, Lindhe J. Periodontal surgery: access therapy. In: Lindhe J, Karring T, Lang NP, eds. *Clinical Periodontology and Implant Dentistry*, 3rd ed. Copenhagen: Munksgaard; 1998:509-549.
- Horton JE, Tarpley TM, Wood LD. The healing of surgical defects in alveolar bone produced with ultrasonic instrumentation, chisel and rotary bur. *Oral Surg Oral Med Oral Pathol* 1975;39:536-546.
- Spencer P, Payne JM, Cobb CM, et al. Effective laser ablation of bone based on the absorption characteristics of water and proteins. *J Periodontol* 1999;70:68-74.
- Lewandowski KU, Lorente C, Schomacker KT, Flotte TJ, Wilkes JW, Deutsch TF. Use of the Er:YAG laser for improved plating in maxillofacial surgery: Comparison of bone healing in laser and drill osteotomies. *Lasers Surg Med* 1996;19:40-45.
- el Montaser MA, Devlin H, Sloan P, Dickinson MR. Pattern of healing of calvarial bone in the rat following application of the erbium-YAG laser. *Lasers Surg Med* 1997;21:255-261.
- Nelson JS, Orenstein A, Liaw LH, Berns MW. Mid-infrared erbium:YAG laser ablation of bone: The effect of laser osteotomy on bone healing. *Lasers Surg Med* 1989;9:362-374.
- Spencer P, Cobb CM, McCollum MH, Wieliczka DM. The effects of CO₂ laser and Nd:YAG with and without water/air surface cooling on tooth root structure: Correlation between FTIR spectroscopy and histology. *J Periodont Res* 1996;31:453-462.
- Williams TM., Cobb CM, Rapley JW, Killoy WJ. Histologic evaluation of alveolar bone following CO₂ laser removal of connective tissue from periodontal defects. *Int J Periodontics Restorative Dent* 1995;15:497-506.
- Baker PJ, Rotch HA, Trombelli L, Wiskesjö UME. An in vitro screening model to evaluate root conditioning protocols for periodontal regenerative procedures. *J Periodontol* 2000;71:1139-1143.

Correspondence: Dr. Katia Miyuki Sasaki, Division of Periodontology, Department of Hard Tissue Engineering, Graduate School, Tokyo Medical and Dental University, 1-5-45, Yushima, Bunkyo-Ku, Tokyo 113-8549, Japan. Fax: 81-3-5803-0196; e-mail: sasaki.peri@tmd.ac.jp.

Accepted for publication January 11, 2002.